

## ELECTRON DENSITIES OF HII REGIONS THROUGHOUT THE NGC 6946 DISK

J. E. Beckman,<sup>1,2,3</sup> B. Cedrés,<sup>1,3</sup> C. Giammanco,<sup>4</sup> A. Bongiovanni,<sup>1,3</sup> and J. Cepa<sup>1,3</sup>

### RESUMEN

Hemos usado el filtro sintonizable de OSIRIS para observar las líneas del doblete de [SII] a  $\lambda\lambda 617.7$  and  $673.1$  nm en emisión a través del disco de NGC 6946, y estimado la densidad electrónica in situ de 387 regiones HII hasta el momento. Los valores muestran un declive constante entre  $350 \text{ cm}^{-3}$  a  $\sim 1/3 R_{25}$  y cerca de  $175 \text{ cm}^{-3}$  a  $2/3 R_{25}$ .

### ABSTRACT

We have used the tuneable filter system of OSIRIS to observe the [SII] doublet lines at  $\lambda\lambda 617.7$  and  $673.1$  nm in emission across the full face of NGC 6946, and estimated the in situ electron densities for 387 HII regions, so far. The values decline steadily from over  $350 \text{ cm}^{-3}$  at  $\sim 1/3 R_{25}$  to around  $175 \text{ cm}^{-3}$  at  $2/3 R_{25}$ .

*Key Words:* HII regions — galaxies: individual: NGC 6946 — galaxies: spiral

We used the OSIRIS tuneable filter (Cepa et al. 2003) to scan the [SII] doublet lines at  $671.7$  nm and  $673.1$  nm in emission across the full disc of NGC 6946. The observations were carried out on the nights of August 22nd to 24th 2011 under seeing conditions varying between  $0.5''$  and  $0.8''$ . Sky subtraction was performed by interleaving the pointings on the galaxy with three sky fields displaced N, S, and W by  $12'$ . To allow for curvature of the surfaces of constant wavelength in the focal plane and to cover the full  $8'$  field, the spectral region was observed in 19 “slices”, between central wavelengths of  $670.4$  nm and  $681.2$  nm, at intervals of  $0.6$  nm and with a FWHM of  $\sim 1.3$  nm. Each slice comprises 6 images, 3 on the galaxy and 3 on the sky. The total exposure time for the whole data set was 5130 s. Data reduction followed reasonably standard procedures, using combinations of dome flats and sky flats. Each set of 3 sky images was combined into a single image, and the galaxy sets likewise; in the latter case the astrometry used sharp galaxy sources plus their ghosts for alignment. These combined images were then used to give a sky-subtracted image for each slice. A “deep” image was produced by summing all 19 slices. The continuum was subtracted using the mode of the slices, scaling this to the “deep” image,

and subtracting the two, giving a “detection” image, with the line emission from 847 HII regions. With the positions and extensions of the HII regions determined, their fluxes were extracted slice by slice, using *Sextractor*. The wavelength  $\lambda$  for a given HII region at a radial distance  $r$  (in arcmin) from the centre of the field in a given slice was found, (González et al. 2012) relative to the central wavelength  $\lambda_c$ , from the expressions:

$$\lambda = \lambda_c - 5.04 r^2 + a_3 \lambda^3, \quad (1)$$

where

$$a_3 = 6.0396 - 1.5698 \times 10^{-3} \lambda + 1.0024 \times 10^{-7} \lambda^2. \quad (2)$$

Using all the slices, a “pseudospectrum” for a given HII region, showing the [SII] doublet lines could be produced (see Figure 1 for examples). Using the line ratios for the 387 HII regions with lines sufficiently well deblended and of sufficient S/N to measure them, we made preliminary estimates of the in situ electron density  $n_e$  and plotted these as functions of HII region radius,  $r$ , and of the galactocentric radius,  $R$ . To a first approximation the values of this parameter show no trend with HII region radius. This is in contrast to the mean electron density  $\langle n_e \rangle$ , (shown by Gutiérrez & Beckman (2010) to vary as  $r^{-1/2}$ ), not unexpectedly as  $n_e$  is a property of the dense cooler clumps. However  $n_e$  does fall with galactocentric radius according to:

$$n_e = 580 - 680(R/R_{25}), \quad (3)$$

in units of  $\text{cm}^{-3}$ , where  $580 \text{ cm}^{-3}$  is the projected value of  $n_e$  on the central axis.

<sup>1</sup>Instituto de Astrofísica de Canarias, C/ Vía Láctea s/n, 38200 La Laguna, Tenerife, Spain.

<sup>2</sup>Consejo Superior de Investigaciones Científicas, Spain.

<sup>3</sup>Departamento de Astrofísica, Universidad de La Laguna, 38205 La Laguna, Tenerife, Spain.

<sup>4</sup>Università di Roma Tor Vergata, Dipartimento di Ingegneria Elettronica, Via del Politecnico, 1 00133, Roma, Italy.

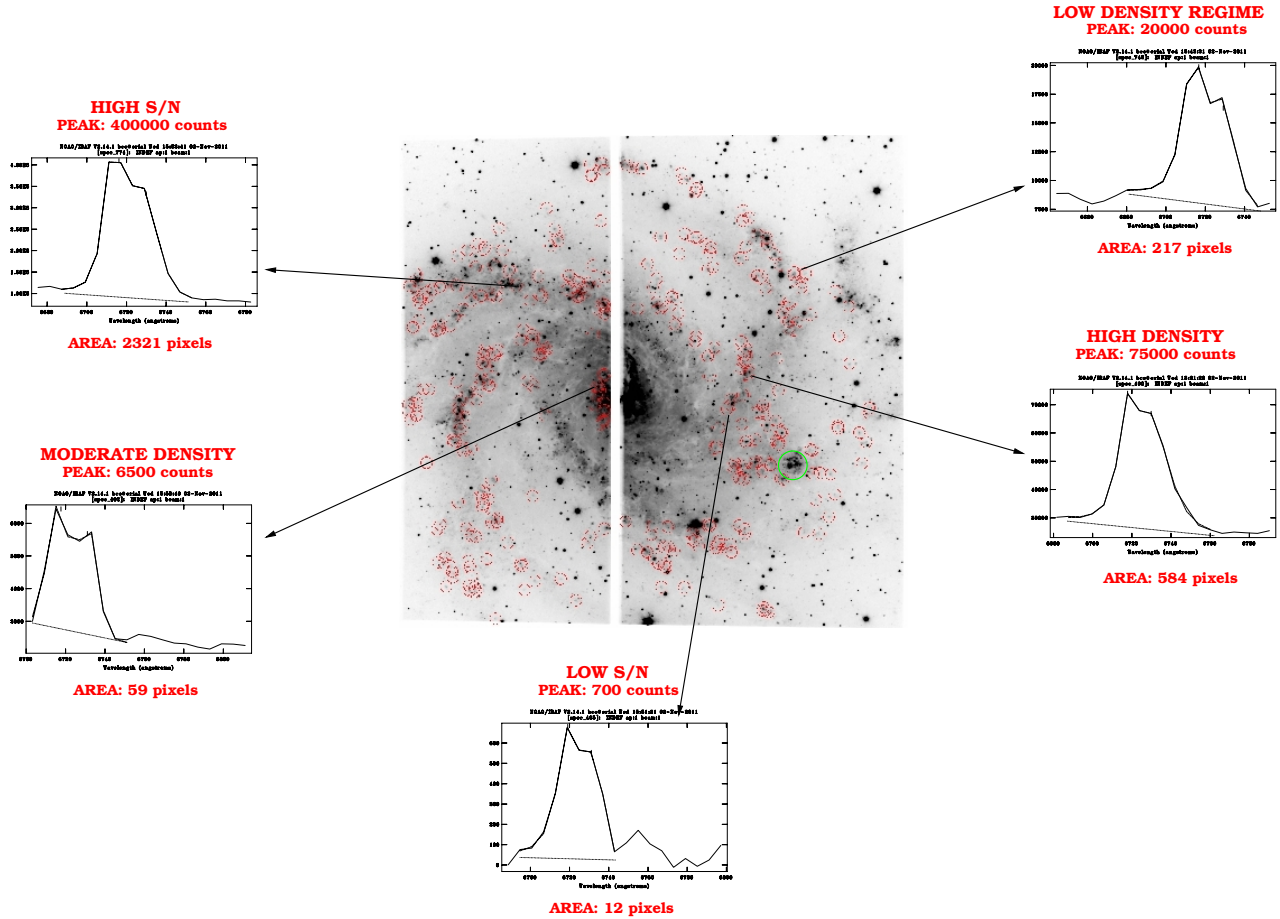


Fig. 1. Image of the galaxy NGC 6946, using a synthetic, custom filter, by co-adding all the slices in the scanned spectral range. The red circles indicate the position of the detected H II regions where the [SII] doublet was debledned. The green circle indicates the position of the giant H II region NGC 6946-1347, which is a reserved target of the OSIRIS guaranteed time (not be studied here). Several “pseudospectra” for selected H II regions are shown. Clockwise from top right, we show the “pseudospectrum” of an H II region in the low density regime ( $n_e < 100 \text{ cm}^{-3}$ ), a high density region ( $n_e=950 \text{ cm}^{-3}$ ), a low signal to noise region, with a maximum peak of just 700 counts, a region with moderate density ( $n_e=450 \text{ cm}^{-3}$ ), and a region with good signal to noise, with a peak well over 400000 counts and an area of 2321 pixels. We note that the a “pseudospectrum” is a convolution of the real spectrum from the H II regions and the response of the instrument OSIRIS, an Airy function. As a first approximation, the profile of the [SII] lines can be fitted using a Voigt function. However, in order to obtain a better debrending and more reliable values for the density, it will be necessary to deconvolve the “pseudospectra”, which is work in progress.

Further work in progress will refine these results.

The authors wish to thank the staff of the GTC, and in particular Dr. Antonio Cabrera Lavers for his help during the observations and reduction of the data. This work was supported by the Spanish Plan Nacional de Astronomía y Astrofísica under grants

AYA2007-67625-CO2-01 and AYA2008-06311-CO2-01.

## REFERENCES

- Cepa, J., et al. 2003, Proc. SPIE, 4841, 1739  
 González, J. J., et al. 2012, ApJ, submitted  
 Gutiérrez, L., & Beckman, J. E. 2010, ApJ, 710, L44